Plant–insect and –fungal interactions in Taxodium-like wood fossils from the Oligocene of southwestern China

Weiyudong Deng, Dario de Franceschi, Xiaoting Xu, Cédric del Rio, Shook Ling Low, Zhekun Zhou, Robert Spicer, Lili Ren, Raoqiong Yang, Yimin Tian, et al.

Plant–insect and –fungal interactions in Taxodium-like wood fossils from the Oligocene of southwestern China

Weiyudong Deng, Dario De Franceschi, Xiaoting Xu, Cédric Del Rio, Shook Ling Low, Zhekun Zhou, Robert A. Spicer, Lili Ren, Raoqiong Yang, Yimin Tian, Mengxiao Wu, Jiucheng Yang, Shuiqing Liang, Torsten Wappler, Tao Su

PII: S0034-6667(22)00067-7

DOI: https://doi.org/10.1016/j.revpalbo.2022.104669

Reference: PALBO 104669

To appear in: *Review of Palaeobotany and Palynology*

Received date: 8 January 2022

Revised date: 5 April 2022

Accepted date: 13 April 2022

Please cite this article as: W. Deng, D. De Franceschi, X. Xu, et al., Plant–insect and –fungal interactions in Taxodium-like wood fossils from the Oligocene of southwestern China, *Review of Palaeobotany and Palynology* (2021), https://doi.org/10.1016/j.revpalbo.2022.104669

Plant-insect and -fungal interactions in *Taxodium*-like wood fossils from the Oligocene of southwestern China

Weiyudong Deng[a,b,c], Dario De Franceschi[d], Xiaoting Xu[a,g], Cédric Del Rio[d], Shook Ling Low[a], Zhekun Zhou[a], Robert A. Spicer[a,h], Lili Ren[e], Raoqiong Yang[a,g], Yimin Tian[f], Mengxiao Wu[a,g], Jiucheng Yang[a,f], Shuiqing Liang[a], Torsten Wappler[b,c,*], Tao Su[a,*]

[a] CAS Key Laboratory of Tropical Forest Ecology, Xishuangbanna Tropical Botanical Garden, Chinese Academy of Sciences, Mengla 666303, Yunnan, China

[b] Department of Natural History, Hessisches Landesmuseum Darmstadt, Darmstadt 64283, Germany

[c] Paleontology Section, Institute of Geosciences, Rheinische Friedrich-Wilhelms Universität Bonn, Bonn 53115, Germany

[d] CR2P - Centre de Recherche en Paléontologie - Paris - MNHN - Sorbonne Université - CNRS, 43 Rue Buffon, Paris 75005, France

[e] Beijing Forestry University, Beijing 100083, China

[f] Faculty of Land Resource Engineering, Kunming University of Science and Technology, Kunming 650093, Yunnan, China

[g] University of Chinese Academy of Sciences, Beijing 100049, China

[h] School of Environment, Earth and Ecosystem Sciences, The Open University, Milton Keynes MK7 6AA, UK

*Authors for correspondence.

Torsten Wappler (e-mail: torsten.wappler@hlmd.de) and Tao Su (e-mail: sutao@xtbg.org.cn)

Abstract

Cupressaceae fossil tree stumps from the early Oligocene Lühe coal mine in southwestern China contain abundant quartz-petrified damage traces. The wood fossils were assigned to *Taxodioxylon* (very similar to extant *Taxodium*) based on wood anatomy analysis. Within the woods, three types of arthropods- and one fungus-mediated ichnofossils LHIF 1–4 (Lühe wood ichnofossils 1–4) were observed. The boring wood types for LHIF 1–3 are comparable to extant longicorn beetles (Cerambycidae), snout beetles (Curculionidae), and wood wasps (Siricidae). The polyporous structured traces of LHIF 4 were attributed to the invasion of stem canker fungus (Polyporaceae). This first-ever report of *Taxodium*-like fossil from the Oligocene of southwestern China points to Yunnan serving as a refugium for some lineage of gymnosperms at that time. Furthermore, the extensive traces of arthropods and fungus discovered from the fossil wood have filled a gap in fossil records for insect herbivory in this region. The wood stumps and decomposers suggest a swamp-like environment. The disappearance of *Taxodium* after the Oligocene supports incremental aridification and changes in winter season temperature conditions, which shifted the late Paleogene mixed deciduous broad-leaved and needle-leaved forest into the present evergreen broad-leaved forest.

Keywords: plant–herbivore interactions, wood fossil, Cupressaceae, Oligocene, climate change

1. Introduction

Larvae of many arthropods, including Coleoptera, Hymenoptera, and Lepidoptera, spend their early life stage boring wood for nesting, self-protection, and food consumption (Lieutier et al., 2004). These arthropods are “architectural experts”, which are capable of creating highly complex “pipeline systems” to cover all their life demands, ranging from tiny (approximately 1 mm diameter) tunnels to larger intersecting channels (Zhang, 2017). These borings cause permanent damage, affecting tree growth by compromising nutrition transport and defense strategies of the host plants, resulting in slower growth or even killing the plants (Lieutier et al., 2004; Hulcr and Dunn, 2011; Villari et al., 2016). In addition to insects, decomposers like mites, springtails, and fungus also play essential roles in the later degradation of living or dead wood. Some decomposers initially parasitize wood, whereas some others are heavily influenced by the arthropod-mediated systems, growth depending on the excrements and the tunnels generated by the wood-borers (Walter and Proctor, 1999; Stokland et al., 2012). The intricate interactions between woods, arthropods, and fungus are crucial to forest ecosystems, which help in recycling and stabilizing the basal parts of food webs (Lonsdale et al., 2008).

Some non-insect borers, like oribatid mites, had a very early origin in the Middle Devonian (Givetian; Norton et al., 1988). But it was not until the Late Devonian that the mite mediated borings were observed within *Prototaxites* (Labandeira et al., 1997). The mite coprolites and borings in seed ferns were found in the Late Carboniferous (Stidd and Phillips, 1982). These findings proved non-insect boring behavior formed before the Permian. Subsequent research has documented possible boring traces by beetles in the Middle Permian (Naugolnykh and Ponomarenko, 2010), and borings contain coprolite and fungal traces as evidence in the Late Permian (Feng et al., 2017; Wei et al., 2019), revealing symbiotic relationships between different arthropods and fungus in deep geological time. Borings from non-coleopteran insects are mostly reported from the Mesozoic, especially during the Cretaceous (e.g., Labandeira et al., 1997, 2014;

McLoughlin and Mays, 2022), as numerous amber and wood fossil studies provide evidence of the upsurge of these arthropods, including wood wasps (Ortega-Blanco et al., 2008), termites (Francis and Harland, 2006), mayflies (Moran et al., 2010), and soldier flies (Han et al., 2022). Compared to the other two eras, there are more damage records from angiosperm wood fossils (Sutherland, 2003; Greppi et al., 2021).

The wood fossils examined in this study were sampled from the Lühe coal mine in southwestern China. Previous research on the Lühe sediments has led to the discovery of numerous fossils, such as woods (Yi et al., 2003), leaves (Ma et al., 2000; Linnemann et al., 2017), and fruits (Ding et al., 2018). Nevertheless, no fossil insects have been discovered so far from the succession. Thus, through the first *Taxodium*-like wood fossil and its internal boring traces, this work provides new insights into the sedimentary environment and herbivorous activities within the Oligocene Lühe flora.

2. Geological settings

The best known Lühe Basin sedimentary exposures are in the Lühe coal mine and Lühe town. Lühe coal mine section (25.15°N, 101.35°E, Fig. 1A, B and C) is located near Chuxiong city, Yunnan Province, southwestern China. The second recognized outcrop in Lühe town (25.14°N,101.37°E, Fig.1 D) is located 2.6 km southeast from the Lühe coal mine. This outcrop has yielded more leaf fossils than the coal mine section.

Based on an early geochronological study, the Lühe coal mine strata were identified as late Miocene and belonging to the Xiaolongtan Formation (Bureau of Geology and Mineral Resources of Yunnan Province, 1996). Hence a series of macro-fossil and pollen research adopted this age assignment. Subsequently, U/Pb dating of zircons within three primary volcanic ash layers in the Lühe town section gave an early Oligocene age (c. 32 ± 1 Ma, Linnemann et al., 2017). $^{40}Ar/^{39}Ar$ dating of primary ash layers from near the base of the Lühe coal mine section gave a similar age

(~33Ma, Li et al., 2020). Most of the coal mine section lies stratigraphically above the Lühe town section and the age is interpreted to span 35 to 26.5 Ma by magnetostratigraphy (Li et al., 2020; Fig. 1D). The fossil woods sampled in this study was preserved in the ~314 m lignite layer (Fig. 1E, "c2" marked), matched to the 380–410 m lithology map presented in Li et al. (2020) (Fig. 1E, "c1" marked). The result indicates the wood fossil-bearing layer is in Chron 10n near the Rupelian-Chattian boundary in the middle Oligocene.

3. Material and methods

The fossil wood is very brittle. The fossil surface and inner boring structures are partly coated or infilled with silica and calcite (or coarse permineralization). In contrast, freshly exposed surfaces reveal undigested wood components (attrinite over textinite, ulminite, suberinite ingredients, terms follow Kus et al., 2020), silica fillings, and carbonates (after acid treatment, Appendix A). A part of the fossil was embedded in epoxy resin before the preparation of thin sections following the usual technique used for petrography, on the three planes used for wood studies (transverse, radial longitudinal, and tangential longitudinal), mounted onto petrographic slides, and polished until the thickness allowed viewing anatomical details. They were then covered by a coverslip using epoxy. These slides were used for the wood description, studied using an Eclipse 80i Nikon microscope, and photographed using a Nikon D300 camera. Terminology of wood anatomy follows the IAWA (International Association of Wood Anatomists) Committee (2004).

Overviews of the damage traces and surrounding wood fragments were photographed by a Nikon D850 camera (Pictures taken by Xiaoting Xu and Weiyudong Deng). Examination of the inner boring traces was using the ZEISS Smart Zoom 5 system. Scans of the internal structure of the boring tunnels were made using by ZEISS Xradia 410 Versa system, and the 3D structures reconstruction were mediated by XM3D Viewer software (Reconstructed by Weiyudong Deng and Ting Tang). All these morphological observations were carried out in the Institutional Center for

Shared Technologies and Facilities of Xishuangbanna Tropical Botanical Garden (XTBG), Chinese Academy of Sciences. Identification of the boring traces and potential herbivores were carefully compared to the database of Beijing Key Laboratory for Forest Pest Control, Beijing Forestry University (Pictures taken by Lili Ren).

The treated slides and the untreated fossil wood specimens stored in the test tube were placed in CR2P (Centre de Recherche en Paléontologie, Paris). The original wood samples were divided into several parts and assigned different labels, each of them contained one or more borings. Several crystalline tunnels were isolated from the host specimens and stored in test tubes to prevent further fragmentation due to oxidation. These specimens are kept in Paleoecology Collections, XTBG.

4. Results

4.1 Systematics for host plant

Family: Cupressaceae Rich. ex Bartl., 1830

Subfamily: Taxodioideae Endl. ex K. Koch, 1873

Genus: ***Taxodioxylon*** Hartig emend. Gothan, 1905

Specimen numbers: LHW-314-1, LHW-314 (1-2).

Repository: Paleoecology Collections, Xishuangbanna Tropical Botanical Garden, Chinese Academy of Science.

Locality: Lühe coal mine, Nanhua County, Yunnan Province, China.

Stratigraphy: Lühe Formation.

Geological age: Oligocene (Rupelian-Chattian boundary).

Description: Sparsely mineralized and brittle fossil wood (Fig. 2F and G).

Transverse section – tracheids elliptic to rectangular in transverse section (about 900/mm^2 in earlywood), growth ring narrow (0.5 – 1 mm) marked by radially narrow tracheids with thicker walls and dark contents, resin canals absent, diffuse axial parenchyma or in short tangential lines

with dark contents more common in earlywood. Abrupt transition from earlywood to latewood. Latewood with thin- to thick-walled tracheids (double wall larger than radial lumen diameter).

Radial longitudinal section – 1–2 seriate bordered pits in radial walls (predominantly 2 seriate in earlywood), opposite more or less aligned vertically sometimes with crassulae separating pairs of opposite pits, spiral thickening absent. Ray cells with pits in horizontal and vertical thin walls. Cross fields with 1–3 (up to 5) rounded oblique simple taxodioid (? but poorly preserved) pits, in 1 or 2 horizontal rows. Axial parenchyma with dark resinous contents, horizontal walls smooth or slightly nodular.

Tangential longitudinal section – Rays (6) 18 (28) cells high, mainly uniseriate, rarely biseriate.

Resin deposits present in axial parenchyma filling the cell lumina or forming separate bubbles.

4.2 Description of boring types

Four damage types were investigated from the fossil materials, namely LHIF 1–4 (Lühe wood ichnofossils 1–4). All borings were classified by shape, size, and embedded orientation. The potential host insects or other microorganisms were also inferred (see 5.2).

LHIF 1 (Fig. 4): These tunnels are the most common type in the fossil wood. The borings are oriented parallel, or obliquely at approximately 30–45°, to the longitudinal axis of the wood (Fig. 4F). Most of the borings are individually formed inside the wood, without terminal chambers. The length of the LHIF 1 boring type generally ranges from 15–22 mm, only a few specimens are shorter than 10 mm. The cross section varies from circular (1.2–2.2 mm in diameter) to elliptical (long axis: 1.8–2.5 mm, short axis: 1.2–1.5 mm) with reaction rim (Fig. 4B). Some of the tunnels are highly fragmented within the wood (Fig. 4A and D). Exceptionally, some tunnels were easy to separate (Fig. 4E and H), and were distinct by possessing a larger cross section (long axis: 2.0–4.0 mm, short axis: 1.2–2.2 mm), and were long (18–50 mm). The outer surface of the tunnels usually displayed regular parallel ring patterns wrapped by wood sawdust (Fig. 4A and D). Additionally, a helical architecture was also observed with ridges inclined at 30–45° to the tunnel axis (Fig. 4H).

LHIF 2 (Fig. 5A–I): Consists of a tunnel ending with a chamber underneath. The boring tunnel measures approximately 2–5 cm long and 0.8–2.2 mm in diameter, and is embedded perpendicular or slightly oblique to the wood longitudinal axis. The cross section of the tunnel exhibits various shapes from round, ellipse to polylobate (Fig. 5B–H; Appendix A), associated with a gradually increase in diameter from the tunnel cross section through into the chamber (Fig. 5B and C). The inner chamber was completely filled with quartz and calcite, appearing as a narrow oval or spindle shape, with a long axis of 32-55 mm, and a short axis of 5–11 mm (Fig. 5D–H).

LHIF 3 (Fig. 5J–N): This is the most complex boring type present in the fossil wood samples. This architecture comprises three elements: "I", "Y", or "L" -shaped (Fig. 5L–N) modules. The "I" module (Fig. 5L) is much shorter in length and diameter than in LHIF 1. The "Y" (Fig. 5M) module comprises three tunnels connected at 120° (Fig. 5K, with one side broken). The "L" module connects two vertically oriented tunnels, occasionally with one end being sealed (Fig. 5N). The "I", "Y", and "L" combined tunnel structures were relatively small and scattered abundantly within the fossil woods. However, unlike LHIF 1, the LHIF 3 structure can be easily detached from the wood substance. Most of the tunnels were incompletely preserved, and were 0.8–1.2 mm in diameter and shorter than 2 mm in length, making it hard to reconstruct the entire structure of the LHIF 3 type. Every single boring has a smooth surface formed of carbonate, and quartz partially fills the inner part of the cross section.

LHIF 4 (Fig. 6): The ichnofossil was present throughout the entire material of the tree base. Here we used two samples: LHIF 4-1 (Fig.6A) and LHIF 4-2 (Fig. 6F) to describe the traces. The wood piece of LHIF 4-1 is 11.2 × 3.8 cm long and covered with scoop-shaped and grey structures. The majority of these structures exhibit an elongate ellipsoidal shape with 1.5–4 mm long axes, and approximately 1 mm in both depth and width (Fig. 6B and F, "s." marked). Some of the structures were preserved as cobblestone-like or ovoid shapes that were approximately 1 mm long and slightly shorter in depth/width (Fig. 6E). With few exceptions, these structures were aligned parallel to the longitudinal axis of the wood. The "Y1" side (radial section) of the LHIF 4-1 revealed the

multilayered distribution of the damage structures within the tree stumps, like wafer biscuits (Fig. 6C). The "Y2" side of the LHIF 4-1 (Fig. 6D) is polyporous, with single or multiple structures situated in the spongy-like holes, some of the holes are empty. LHIF 4-2 wood piece measured 12.5 × 3.7 cm (Fig. 6F), and illustrates the anatomical structure of the ichno-traces. The "Y" side of LHIF 4-2 displayed more empty holes, and the "Z" side (tangential section) shows the wood matrix after removal of the damaged structures (Fig 6F, "Ep.1" and "Ep.2" show excised surfaces).

To uncover the inner content of tunnels, two samples (LHIF 1) were isolated from the fossil woods for CT scanning and mineralogical study (Fig. 4H; Fig. 7A; Appendix A). The CT scan revealed a quartz-filled inner structure without any frass or sawdust (Fig. 7F). The rough outer rim is clearly separated from the inner structure by a smooth and straight crystallization border, indicating multiple phases of mineralization (Fig. 7B–D). This result provides evidence that the screw-thread-shaped boring tunnel was formed before the mineralization but replaced latterly by quartz and carbonate. The second tunnel that was used for mineralogical study exhibited mainly colorless and clear crystals of α-quartz grains. Furthermore, the sample slightly bubbled during acid treatment at the base of the quartz crystals, which indicates the presence of carbonate minerals, such as calcite (Appendix A).

5. Discussion

5.1 Systematic affinity of the fossil wood

The studied fossil homoxylous conifer woods were partially permineralized. The predominantly uniseriate rays, the rectangular section of tracheids in transverse section, the opposite pits in radial walls, and the presence of parenchyma, all point to the material representing Cupressaceae (*Taxodium*, *Sequoia*, and *Sequoiadendron*) or Podocarpaceae (*Retrophyllum*; Greguss, 1955).

We used the IAWA Committee (Richter et al., 2004) code (40p 42p 45p 46p 72p 73p 74p 78p 80p 98p 104p 107p for this specimen) to interrogate the InsideWood (2004) database (Wheeler et al., 2011). These character states return the following compatible genera: *Taxodium, Sequoia*, and *Sequoiadendron* (*Retrophyllum* is not selected, as there is no description for this genus in the database).

Among Cupressaceae, modern *Taxodium* shows the most similar structure, in terms of the type of transverse end walls of the axial parenchyma cells, ray cells shape and density, and latewood cell wall thickness (characters 54 and 55), as well as the probable absence of secretory canals. The fossil description is therefore fully compatible with the extant genus *Taxodium* (Cupressaceae).

Regarding *Retrophyllum*, the wood of the species *R. minor* (Carrière) C.N. Page (= *Podocarpus minor* Parl. = "bois bouchon" NC, France) which is described and figured in Greguss (1955) and Carlquist and Nazaire (2016), seems also to have some similarity to the Lühe fossil. Carlquist and Nazaire (2016) mentions the presence of "air spaces" attesting to air channels that potentially connect roots to stems. These spaces are seen between ray cells and tracheids, but are not obvious, as checked on *Retrophyllum minor* wood (MNHN Wood collection / from Sorbonne University, number UPMC.239). The fossil wood presents some spaces that could correspond to the description given by Carlquist and Nazaire (2016), but with the current preservation, and the partly disrupted structure caused by pyrite, it is quite difficult to confirm the presence of this character in that it could be an artifact of preservation. According to the studied living sample of *Retrophyllum minus*, the character list for InsideWood DB for living softwood species should be 40p 43p 46p 72p 73p 74p 76p 80p 98p 103p 107p, which also corresponds to several species in Cupressaceae and Podocarpaceae, but is clearly different from the present fossil wood.

The fossil genus *Taxodioxylon* also fits with this description [see Hartig diagnosis (1848), and translation by Philippe and Bamford (2008)]. But this genus includes many fossils from the Jurassic to Pleistocene, from diverse regions of the world, and corresponds (probably) to many extinct and living genera. According to Duan et al. (2020), the concerned clade in Cupressaceae includes not

only *Taxodium* but also *Glyptostrobus*, and *Cryptomeria*. The closest wood structure is found in *Sequoia*, which is at the base of Cupressaceae, together with *Metasequoia*, *Taiwania*, and *Cunnighamia*.

Previous studies reported the discovery of *Taxodioxylon* fossil woods from the Lühe coal mine section. Yi et al. (2003) obtained four calcified wood specimens in the coal mine, two specimens (YNCN101 and YNCN104) were assigned to *Taxodioxylon cryptomeripsoides* Schonfeld 1953, and the others (YNCN102 and YNCN103) were assigned to *Taxodioxylon cunninghamioides* Watari 1948. There is another *Taxodioxylon* fossil from a Lower Cretaceous basin of Jixi, Heilongjiang Province, northeastern China, namely *Taxodioxylon szei* Yang and Zheng, which exhibits a striking similarity with extant *Taxodium* (Yang and Zheng, 2003). The distinct differences between the two samples in Yi et al. (2003) are that *Taxodioxylon cunninghamioides* has occasional biseriate rays visible in tangential section, which is regarded as the identifying feature of modern *Cuninghamia*; while *Taxodioxylon cryptomeripsoides* has mostly one row of bordered pits in radial walls, and rays that are 1–18 cells high. Both samples from Yi et al. (2003) are preserved by calcification, which is distinctly different from the wood fossils in this study. The samples were not assigned to a particular species because the cross-field pits are not clearly observed. Previous studies have also shown *Taxodium* to have distinct nodular structures present on the end walls of axial parenchyma as seen in transverse section (Dolezych and Schneider, 2007; Jiang et al., 2010). However, the "Atlas of Gymnosperms Woods of China" mentioned that "end walls of parenchyma cell smooth" in some species of *Taxodium* (Jiang et al., 2010, p.366), which is consistent with *Taxodioxylon szei* and the wood fossil in this study.

From a taphonomic perspective, the almost non-petrified (terms following Luczaj et al., 2008) fossil tree stumps were conspicuously different from the lignite surroundings. Well preserved non-petrified woods (mummified, humified, non-mineralized, uncoalified, or others) have been found in many open-cast mines worldwide, the product of waterlogged anoxic preservation (Erdei et al., 2009; Luczaj et al., 2018; Mustoe, 2018; Mustoe et al., 2019; Kus et al., 2020). The lignite matrix

surrounding the Lühe wood fossil is very similar to that described for the Meuro coal mine (Kus et al., 2020), which was interpreted as a subtropical mixed deciduous conifer forest mire environment. The quartz-filled boring tunnels within the wood also revealed a long-term waterlogged or high-pressure environment during the sedimentation (Appendix A). Although diagenetic mineral replacement was evident, this was minimal and the largely unaltered wood, is vulnerable to modern fungus, mites, and other arthropods (Appendix A). The living habitat of two tree genera, i.e., *Glyptostrobus* and *Taxodium*, are described as "the only genera of Taxodiaceae to be amphibious" (Kubitzki et al., 1990, Volume I: Pteridophytes and Gymnosperms), consistent with the swamp-like environment inferred from the fossil setting.

In summary, we give *Taxodioxylon* sp., an affinity to extant Taxodiaceae (now in Cupressaceae) as it contains all listed characters of this family (Table1), the result is enough to study the plant-insect interactions. Considering the wood anatomy and inferred habitat, the *Taxodioxylon* sp. wood fossil in this study is most similar to extant *Taxodium*, but less so to *Glyptostrobus*. It shows little resemblance to *Cryptomeria*, *Cunninghamia*, *Sequoia*, *Metasequoia*, *Taiwania*, and the other listed fossil species (Table 1).

5.2 Parasitic arthropods and fungus

Modern Taxodiaceae wood hosts various consumers, including arthropods, fungus, and other decomposers (Wood et al., 2003; Zhou et al., 2013). Arthropods ranging from Lepidoptera, Coleoptera, Hymenoptera, to Hemiptera are widely reported to exploit seeds, leaves, or the wood of Cupressaceae, but few of them are real wood borers (Wood et al., 2003). Lepidoptera, for example, mostly feed on needles and cones (Chen, 1990; Kruse, 2000), or bore into green branches (Ohya and Ogura, 1993), while wood boring families, including Cossidae (Solomon, 1977), Hepialidae (Grehan, 1987), and Sesiidae (Solomon, 1977; Leskey et al., 2009), are seldom reported boring into conifer trees. The majority of the conifer wood borers are Coleoptera and Hymenoptera, including longhorn beetles (Cerambycidae), snout beetles (Curculionidae), jewel bugs (Buprestidae), and wood wasps (Siricidae) (Wood et al., 2003; Lieutier et al., 2004). All these arthropods possess

different boring behaviors, which produce tunnels or chambers within the bark, sapwood, or even heartwood with a variety of architectures. Regarding the *Taxodioxylon* specimen described in this study, four types of damage traces have been identified, generated by arthropods and fungus (Figure 8, remarks: not all the arthropods in the figure are parasitic on Taxodiaceae, the figure only shows similar boring behaviors in arthropod genera).

For LHIF 1, there is no significant excreta (frass) and other content substances, making it difficult to identify the perpetrator definitively. The anatomical structure and the CT scan illustrate the demarcation between the tunnel mineral layer and the outer rim wall (Fig. 7B-D). The result indicates the parallel outer rim structures (Fig. 4H) represent the wall (Fig. 4H, with arrow) as originally built by arthropods. Subsequently, quartz mineralization filled the inner gallery space. Most modern beetle and wood wasp mediated tunnels are embedded within the sapwood and are initially excavated vertically following tree rings (Fig. 8L), and then along fibers (Fig. 8B). Some extant insects produced the screw thread-like tunnel wall architecture, closely related to the tree rings (Fig. 8L) or wood fibers (Fig. 8A and B). For the oblique orientation of tunnels at 30~45° to the wood axis (Fig. 4F), a 30~45° helical arrangement of the tunnel rims was also observed, producing a screw thread appearance (Fig. 4H). There are also some exceptions where the tunnels did not follow these particular directions, but still display the screw thread structures (Fig. 8J). It is possible that secondary processes may have modified the original tunnel wall structure: the frass or sawdust caused by the original arthropods, possibly longicorn beetle or wood wasp larva, were subject to decomposition by mites, springtails, or fungus, which will result in a different gallery wall compared to that originally produced (Fierke et al., 2005). Additionally, some tunnel surface structures (Fig. 4G and H) show clear modern (can be heated to charring) and mineralized (heating does not produce any changes) fungal structures, which indicates fungus had invaded the tunnels after the original bores were formed.

In regard to LHIF 1, we conclude that arthropods, attributable to the extant groups including Anobiidae, Cerambycidae, Curculionidae, Bostrichoidea, Siricidae, and Xylocopidae, are all

possibly the primary insect borers (Zhang, 2017; Fig. 8). These groups include parasitic genera on conifer trees, and most of them produce a similar boring tunnel size and orientation to LHIF 1 (Fig. 8A, B, G, I, and L). As most exhibit a screw thread pattern on the tunnel wall, it suggests arthropods of the Cerambycidae, like *Semanotus*, or *Hylotrupes* may be the potential borer, as their tunnels often show a similar architecture (Fig. 8A, B, and J). Moreover, the Cerambycids may cover the pupal chambers with calcareous layers (Kimoto and Duthie-Holt, 2004; Greppi et al., 2021), although this is not obviously present on the fossil borings, the CT scan reveals the presence of an outer tunnel lining (possibly formed by calcareous materials or degraded organics) that is quite distinct from the inner (secondary) quartz layer (Fig. 7). Some tunnels of *Sirex* (Siricidae), although not showing distinct screw thread structures, are also consistent with the LHIF-1 (Fig. 8K & L).

LHIF 2 is particularly distinct in that it displays a chamber-like structure, with an inter-connected tunnel (Fig. 5). The chamber is an expansion of the initial boring, which was created for pupal development. The tunnel connected to emergence hole for the adult (Fig. 5 A–I). Based on this boring feature, members of the Curculionidae, Cerambycidae, and Siricidae seem to be the most likely arthropods responsible for the borings (Morgan, 1968; Cope, 1984). One extant example for making a similar boring as seen in LHIF 2 is *Eucryptorrhynchus* (Curculionidae, Fig. 8H), where the newly hatched larva conducts their activities in the bark and later move deeper into the sapwood. The tunnels expand with the growth of the larva and end with the pupal chamber. After the chamber is formed, the larva starts boring vertically and creates an emergence hole larger in cross section than the early-stage boring (Description translated from Zhang, 2017, Fig. 8E). The orientation of the emergence hole seen in the fossil coincides with the boring behavior of *Eucryptorrhynchus* (Fig. 8H). Regardless of the direction of the chamber formed (horizontal, vertical, or multi-direction) in modern wood, the emergence hole for the mature larva was always orientated vertically and situated on the top of the chamber (Fig.5 A–I; Fig. 8E).

LHIF 3 comprises different shapes of modules that form intricate tunnel systems. These tunnels are shorter in length and smaller in diameter than LHIF 1. Furthermore, they display no

specific orientation and have a smooth gallery wall. Abundant invasion holes of LHIF 3 were observed on the bark, representing a high density of arthropods present in this tree. The LHIF 3 appears to have been produced by small Coleoptera without any preference for boring orientation and the ability to build complex connected tunnels. Today cerambycid (longhorn), scolytid (bark), and buprestid (jewel or metallic wood-boring) beetles produce similar tunnels (Fig. 8A, C, D, and J). *Xylotrechus* (Cerambycidae), for example (Fig. 8B and G), forms intersecting tunnels when there is a high density of insect activity in the same host plant, and track fiber direction, turning soon after the invasion hole and before the emergence hole (Fig. 8A). *Xylotrechus* shares similar characteristics to those of the fossils in terms of the tunnel shape, its location in the inner sapwood and abundant holes on the bark. However, most beetles, including *Xylotrechus*, are larger than those of the Buprestidae, and produce tunnels 1.5–3 times wider in cross section than are produced by the Buprestidae (Zhang, 2017). Moreover, the internal walls display screw thread structures, which contrast with the smooth linings of LHIF 3. Because of this, insects attributable to the Buprestidae are better candidates as producers of the fossil borings (Fig. 8D). The borings in the sapwood form a cross or bifurcate-shaped tunnels perpendicular or parallel to the long axis of the wood, and the tunnel size is comparable to those seen in LHIF-3 as most of the Buprestidae are relatively small. Because most of the tunnels are incomplete in LHIF-3, there is another possibility that these tunnels are just some branches of the main tunnel caused by Scolytinae (Fig. 8C, “M.” and “S.” marked; subfamily of Curculionidae).

It is difficult to determine whether LHIF 4 was caused by animal boring, or by fungal decomposition. This type most likely represents partially rotted wood (Fig. 8M) filled with carbonates during deposition. Genise et al. (2004; 2012) lists two similar ichnospecies belonging to the ichnogenus *Asthenopodichnium* Thenius, 1979: *A. xylobiontum* and *A. lignorum*. The ichnogenus is described as “small U-shaped structures in the wood”, “pouch-like structures in wooden, organic substrates”, or “as a mass of tongue filled structures, non-xylic material” (Thenius and Klaus, 1978; Genise et al., 2012). These two types of ichnospecies generally follow the

description of *Asthenopodichnium* in terms of appearance, shape, and arrangement, but have distinctly different inducers and paleoenvironment backgrounds. Most studies have attributed *A. xylobiontum* to typical mayfly nymphs (Ephemeroptera) boring traces (Moran et al., 2010), likely from Polymitarcidae or Palingeniidae (Kluge, 2013). Some have doubted that the traces were formed by fungi or animals at all (Genise, 2004; Uchman, 2011). On the other hand, *A. lignorum* is believed to represent fungal mediated traces. Genise et al. (2004) listed several fossil sites far from the influence of Polymitarcidae and Palingeniidae in geological time and noted inconsistencies between shapes produced by the larvae and the "U-shaped" tunnels in both fossil wood and sediments.

The architecture of LHIF 4 appears very similar to that described in the diagnosis for *Asthenopodichnium*, but displays some distinct characteristics in both size and color. The type of *A. xylobiontum* caused by mayfly families is considered Asiatic in origin (Genise et al., 2012), and thus relevant to our samples. Nevertheless, the LHIF 4 ichnofossils are smaller, more rounded, and arranged more densely than *A. xylobiontum*. This covers the wood slide like a "wafer biscuit" (Fig. 6C). On isolating these structures, each presents with parallel stripes that may relate to wood fiber (Fig. 6F, "S." marked). Thus, compared to *A. xylobiontum*, the differences seen in LHIF 4 may possibly be because of the depositional condition of the wood fossil, as the samples in this study were not replaced by minerals and unlike silica rinds, iron hydroxide, or sandstone casts, the preservation of the structures is mainly filled with quartz, calcite, or other carbonates, leading their white to grey color. Second, the borings may not have been caused by insects or other animals, but by fungus. Although some of the characteristics of LHIF 4 are also different to *A. lignorum* (Genise et al., 2012), the shapes and the arrangements are similar, and likely to be due to stem canker fungus as the structures are commonly observed in other wood fossils collected from the Lühe coal mine.

LHIF 1–4 indicates the woods represented within the Lühe floras encountered a variety of consumers both during life and afterward. Arthropods ranging from Cerambycidae, Curculionidae, Bostrichoidea, Buprestidae, and Siricidae are all possible damage inducers. At least four (Fig 4G,

LHIF 4, and Appendix A) different ancient and extant fungi took part in the degradation progress. The relationships between the different arthropods and fungi are not clear because of the wood preservation condition.

5.3 Paleoenvironment implication

The wood anatomy reveals strong seasonal contrasts in growth with sharp contrasts between early wood production and late wood, which in this Oligocene thermal regime at this latitude points to synchronous obligate shedding of leaves (i.e. the tree was deciduous) and the tree stump context shows it inhabited a swampy environment. Notably, the nearest living relative of the tree producing the wood lives this in kind of environment (e.g., *Taxodium*) and is deciduous. The paleoenvironment represented by the outcrop seems to have been a subtropical environment with a marked rainy season, forming a seasonally flooded swamp forest but with a distinct dryer season.

The inferred hosted arthropods in this study today mostly possess a wide distribution in tropical and temperate regions, constrained by the extant distribution of conifer trees. However, *A. lignorum*, the similar fungus related type to LHIF 4, inhabited humid to semi-humid environments, based on comparison with the modern terrestrial environment in Argentina (Genise, 2004; Genise et al., 2012). The abundant consumer traces but low degradation condition, the quartz tunnel infill (formed after deposition), and the lignites, all indicate a waterlogged swamp-like environment during the deposition formation.

Besides the *Taxodium*-like wood fossil in this study, the discovery of other 4 types of Taxodiaceae (now in the Cupressaceae) fossils in the Oligocene Lühe succession (Ma et al., 2000; Yi et al., 2003), together with the *Metasequoia* that occurs in the Miocene Sanzhangtian and Maguan assemblages had both shown the existence of relict plants in southwestern China (Ma et al., 2000; Zhang et al., 2015; Wang et al., 2019). Wang et al. (2019) mentioned *Metasequoia* as an important forest element in much of the Northern Hemisphere after the Late Cretaceous, but subsequently retreated during the Neogene. Study of *Sequoia* also revealed a wide distribution during the Late Cretaceous in northern China, but is represented only by fossil records during the

Cenozoic in both the northern and eastern parts of China (Zhang et al., 2015). This points to southwestern China as a refugium for the Cupressaceae during the Cenozoic. The intensification of monsoonal climate, characterized by increased seasonality of precipitation, may explain the absence of *Sequoia* and *Metasequoia* in modern forests of Yunnan (Zhang et al., 2015; Wang et al., 2019). This is also the case for *Cedrus* in this region (Su et al., 2013).

Previous paleoenvironmental reconstructions based on macrofossil and palynological samples from the Lühe town section showed floristic differences between the early Oligocene flora and that seen there today (Linnemann et al., 2017). Tang et al. (2020) reconstructed a deciduous broad-leaved mixed conifer and evergreen broad-leaved forest for Lühe in the Oligocene and suggested the vegetation was influenced by cold winter temperatures. The shift from deciduous mixed forest elements to the modern evergreen dominated forest indicates a temperature increase following the Yunnan–Guizhou Plateau uplift (Tang et al., 2020). Tang et al. (2020) also revealed no significant floristic changes during the Eocene–Oligocene transition (EOT), where no abrupt regional changes happened to plant community composition despite more global climatic changes recorded in deep sea sediments. For the coal mine section, biomarker analysis shows no marked cooling, which is similar to results from the town section (Lauretano et al., 2021, under review). Elsewhere in the nearby region, such as in Markam (Su et al., 2019; Deng et al., 2020) and Jianchuan (Wu et al., 2018), interpretations of climate and vegetation changes across the EOT are complicated because of possible contemporaneous regional uplift. While it seems that heterogenous EOT climate changes took place worldwide, regional environment in southwestern China appears to have been relatively stable. Compared to the complex temperature differences across the region, the precipitation interpreted from most Neogene floras are strikingly similar, showing a pronounced higher annual precipitation compared to the modern environment (Sun et al., 2011). Most importantly, modern precipitation during the dry season is much less than was the case in the Oligocene (Sun et al., 2011; Tang et al., 2020), which could explain the loss of the Cupressaceae and other relict plants here (Huang et al., 2015).

To conclude, the *Taxodium*-like deciduous Cupressaceae fossil wood in the coal mine, together with other reported fossil Cupressaceae genera in Yunnan Province, represent relict plants that once dominated the Northern Hemisphere during the Late Cretaceous and Paleogene. The Neogene retreat constrained their distribution in southwestern China, and the modern absence of the species in the fossil region related to further temperature and precipitation changes during the Neogene in southwestern China. From the early Oligocene onwards, colder winter temperatures led to coniferous-broad-leaved mixed forest in the region (Tang et al., 2020). The relatively high precipitation during the growing season allowed the development of a swamp environment, guaranteeing the habitat of *Taxodioxylon* (Fig. 9A–F). The mass arthropod and fungi traces also prove evidence for abundant consumption and decomposition in the region. The tree base was buried within a waterlogged environment, making the main structure almost non-petrified and inner boring tunnels mineralized. The surrounding organic matter accumulated and decomposed as lignite, with higher rank sub-bituminous coals being restricted to the deeper parts of the Lühe mine (Fig. 9B). Over time, some original Cupressaceae and deciduous elements were replaced by the evergreen taxa, forming the modern evergreen broad-leaved dominated forests of the region (Fig. 9C).

6. Acknowledgments

We thank Vincent Rommevaux for the delicate work of wood section slide preparation; Anaïs Boura for providing original wood anatomy pictures of *Retrophyllum*; Hong Liu and Shuyin Li for providing extant *Taxodium* pictures images from South–Central University for Nationalities; Carlos D. Greppi for providing references. We thank the Institutional Center for Shared Technologies and Facilities, XTBG, for facilities accessed of micro-CT scan and technical support, particularly Ting Tang for the assistant on computerized tomography. This work is supported by the National Natural Science Foundation of China (Nos. 42072024, 41988101, 41922010); Second Tibetan Plateau

Scientific Expedition and Research Grant (No. 2019QZKK0705); the Strategic Priority Research Program, CAS (Nos. XDA 20070301, XDB 26000000); and Sino–German (CSC–DAAD) Postdoc Scholarship Program (No. 57575640).

Figure 1 (A) Locality of the Lühe basin. **(B)** Geological context of Lühe coal mine and Lühe town section. Black star = Lühe coal mine section; white star = Lühe town section. (modified from Li et al., 2020). **(C)** Panoramic view of Lühe coal mine section. **(D)** Panoramic view of Lühe town section. **(E)** Position of the studied wood fossil in the coal mine (indicated by a star), and a brief lithology comparison between different sampling sites. "C1" = Coal mine section 1 (Li et al., 2020). "C2" = Coal mine section 2 (this study). "T." = Town section.

Figure 2 (A–E) Different wood fossils preserved in Lühe coal mine section, A and B is embedded in a lignite layer, C is embedded in a siltstone layer. D and E represent lignified and coalified wood. **(F–G)** Some of the fossil wood that contains tunnel like ichnofossils. (Scale bar = 1cm)

Figure 3 *Taxodioxylon* sp. **(A)** Transverse section. **(B)** Zoom of transverse section and tracheids. **(C)** Detail of parenchyma. **(D)** Tangential longitudinal section. **(E–F)** Radial longitudinal section. **(G–H)** Cross fields. (Scale bars, A= 500μm; B & D = 100μm; C, E & H = 50μm)

Figure 4 (A) Boring tunnel across bark and sapwood. "st" = screw thread-like paralleled structures. "tc" = tunnel cross section. **(B)** Zoom of round, crystal filled boring tunnel cross section, "r" = reaction rim. **(C)** Detail of the irregular tunnel cross section. **(D–E)** Mineralized boring tunnels embedded in wood. **(F)** Detail of hollow tunnel cross section. **(G)** Detail of photo H, attached fungus (Modern and silica formed fossil). **(H)** An excised mineralized tunnel, parallel outer rim, 30~45° helix angle. (A–H: LHIF 1; Unmarked scale bar = 1cm)

Figure 5 (A) Structure of a chamber contained within the wood. **(B–C)** Detail of photo D and E, respectively. "tc" = tunnel cross section. **(D–H)** "Y" angle of the boring chamber cross section. **(I)** A tunnel connected boring chamber. "t" = tunnel, "eh" = emergence hole, "bc" = boring chamber. **(J)** Multi-connection tunnels, forming a web structure in the wood. **(K)** Detail of photo J, "cp" = conjunction part. **(L–N)** Module of the multi-connection tunnels, including "I", "Y", and "L" shape. (A–H: LHIF 2; I–N: LHIF 3; scale bar = 1cm)

Figure 6 (A) LHIF 4-1, radial section. **(B)** Detail in of LHIF 4-1, calcite filled polyporous structures. **(C)** "Wafer biscuit" like appearance between damage traces and woody substrate. **(D)** Another "Y" side of LHIF 4-1. **(E)** Detail of one calcite filled scar. **(F)** LHIF 4-2 anatomy; "ep 1 & 2" = excised parts of 1 & 2; "s" = separated single structure. (Unmarked scale bar = 1cm)

Figure 7 (A) CT scan of the tunnel. "rs" = radiation Sources, "cs" = camera system. **(B-E)** Different angle of the scan. Obvious separation between outside and inner mineral layers. **(F & G)** Reconstruction 3D structures.

Figure 8 (A) Extant *Xylotrechus grayii* in *Fraxinus pennsylvanica*. "st" = screw thread structure. **(B)** *Xylotrechus magnicollis* in *Koelreuteria bipinnata*. **(C)** *Callidium villosulum* and *Phloeosinus sinensis* in *Cunninghamia lanceolata*. "m" = mother (or main) tunnel, "f" = frass, "s" = sub-tunnels. **(D)** *Agrilus planipennis* in *Fraxinus pennsylvanica*. "ct" = crossed tunnels. **(E)** *Eucryptorrhynchus brandti* in *Ailanthus altissima*. "eh" = emergence hole, "bc" = boring chamber. **(F-I)** *Callidium villosulum*, *Xylotrechus magnicollis*, *Eucryptorrhynchus brandti*, and *Sirex noctilio*. **(J)** Same with photo A. **(K & L)** *Sirex noctilio* in *Pinus sylvestris*, "i" = invasion hole; "tr" = tree ring; "t" = tunnel. **(M)** Mangrove bored by *Sphaeroma* (not matched to LHIF 4, just to show general appearance of polyporous canker wood).

Figure 9 (A) Extent habitat of *Taxodium distichum* (Estimated landscape of Oligocene Lühe flora). **(B)** Landscape of modern Lühe flora (Photo from Zixi Mountain, Yunnan). **(C)** Lühe coal mine. **(D)** Introduced *Taxodium distichum* (Photo from South Central University for Nationalities, Hubei). **(E)** "I" = invasion hole. **(F)** Dead tree base. "tb" = tree base.

Table 1 Anatomical structure comparison between different species from Cupressaceae.

Appendix A (A) Inner tunnel structure formed by quartz and calcite. **(B)** 10% HCL treated sample after 30 minutes reaction time, no obvious bubbles, main structure of mineral without any changes, evidencing quartz. **(C)** 10% HCL treated sample, some bubbles indicate the presence of calcite. **(D)**

Separated wood components and silica. **(E–H)** Modern decomposers separated out after the acid treatments (All modern samples can be burned and turned black after prolonged acid treatment). **(I–L)** Different types of tunnel cross sections, from mineral to sawdust formed gallery wall. I: LHIF 3, tunnel gallery with a smooth wall; J: LHIF 1, tunnel wall with regular rings; K: LHIF 1, tunnel wall with sawdust remains. L: LHIF 2, tunnels within the wood structure. (Unmarked scale bar = 1mm)

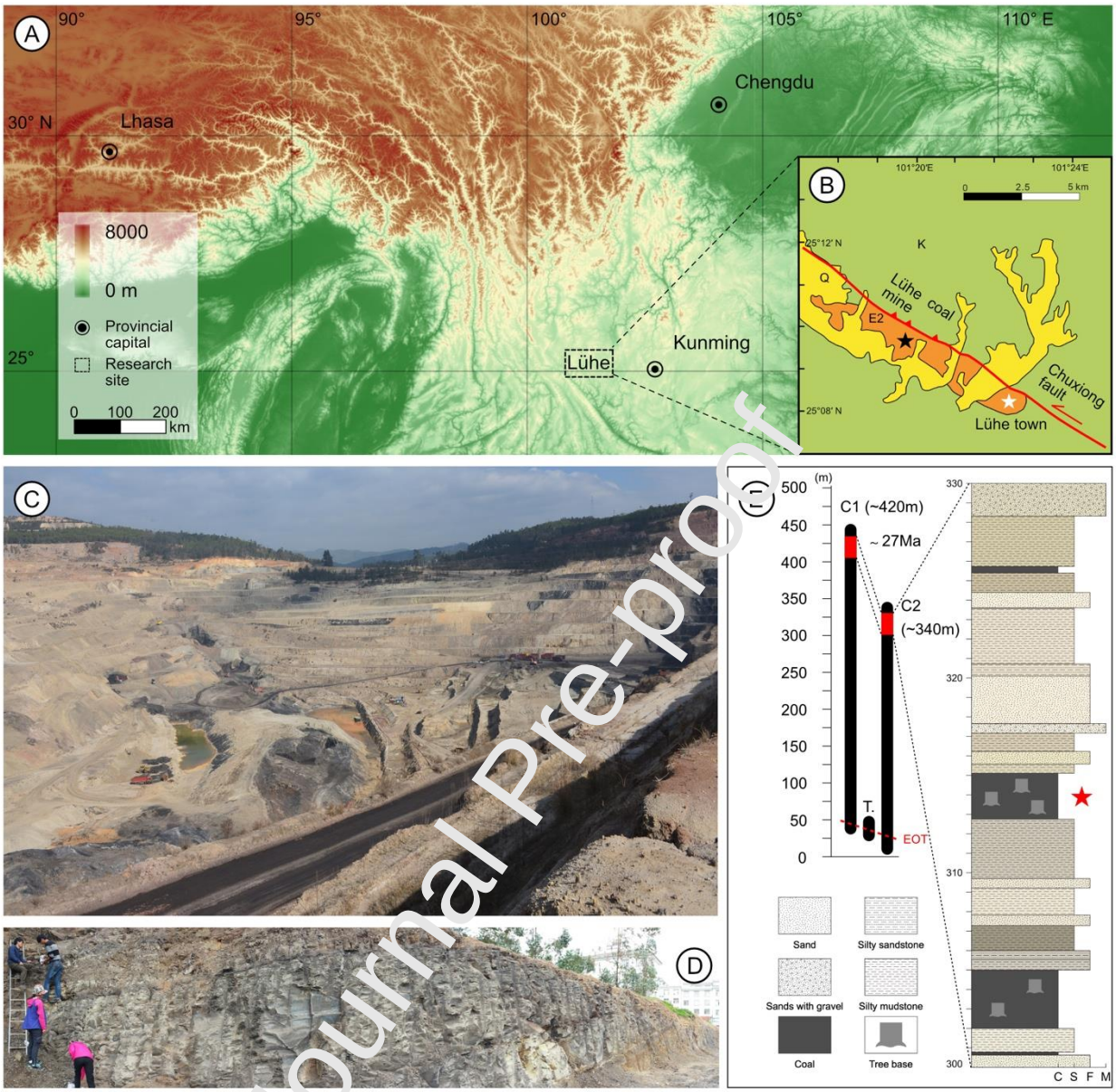

Figure 1

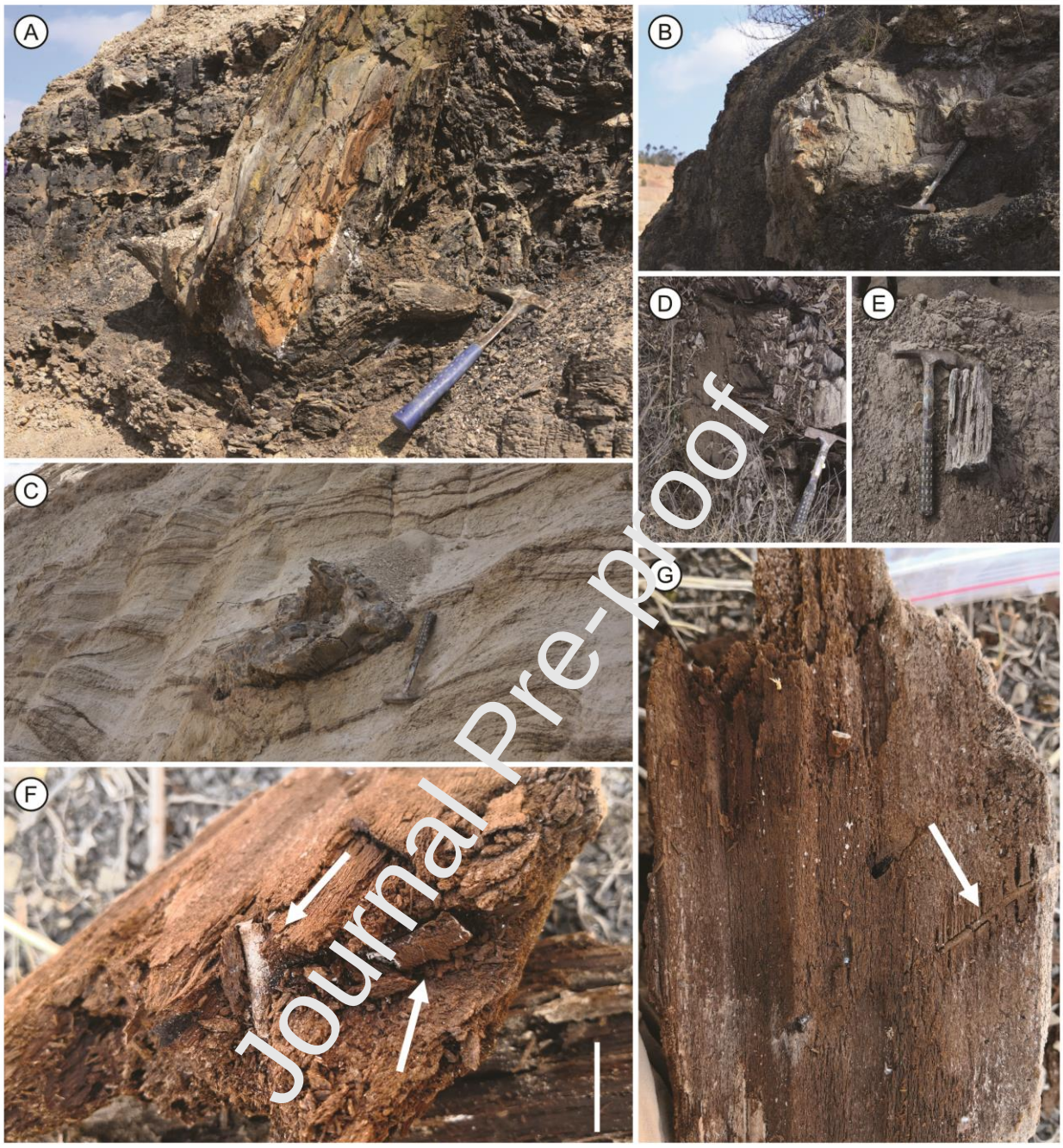

Figure 2

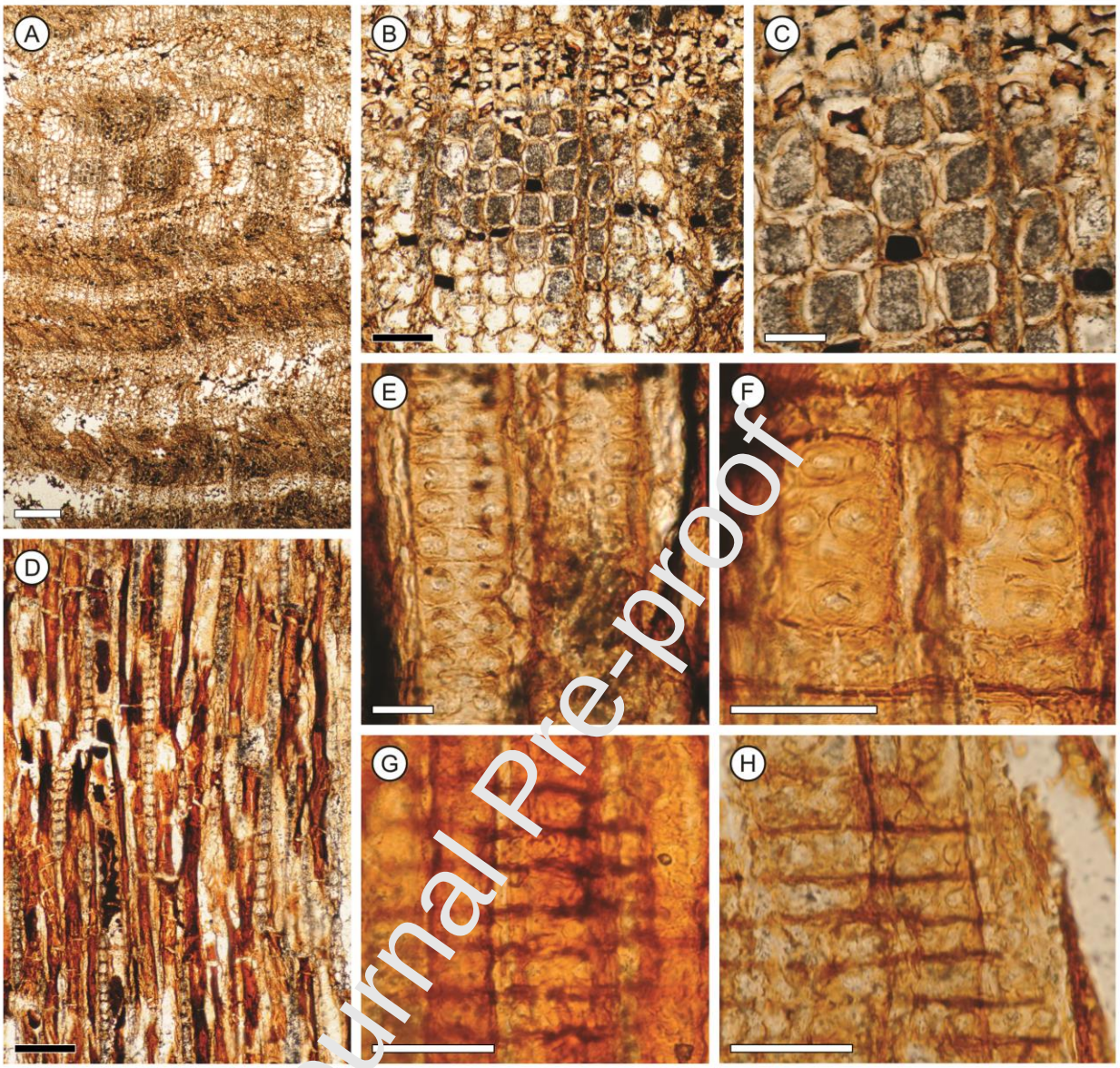

Figure 3

Figure 4

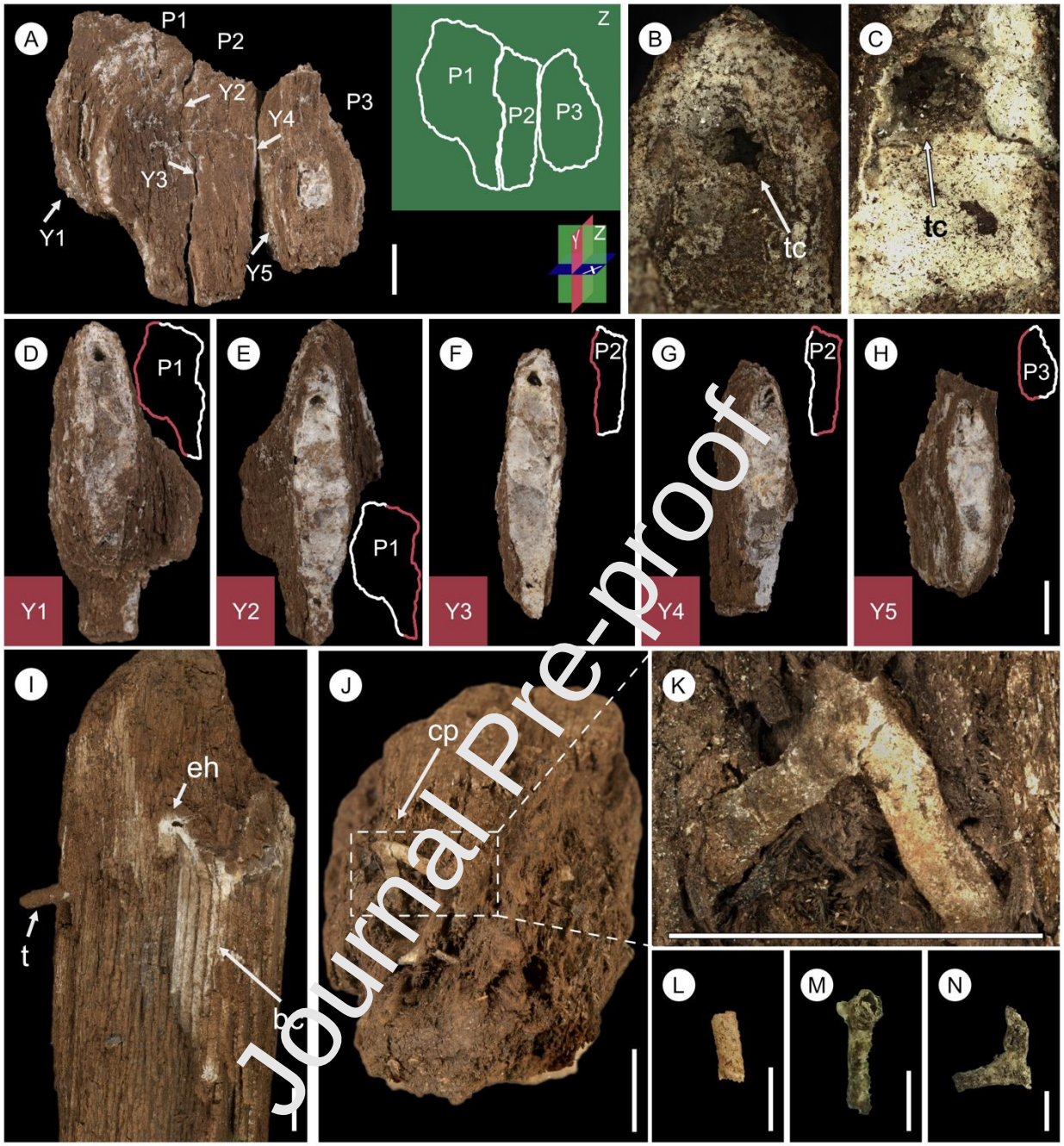

Figure 5

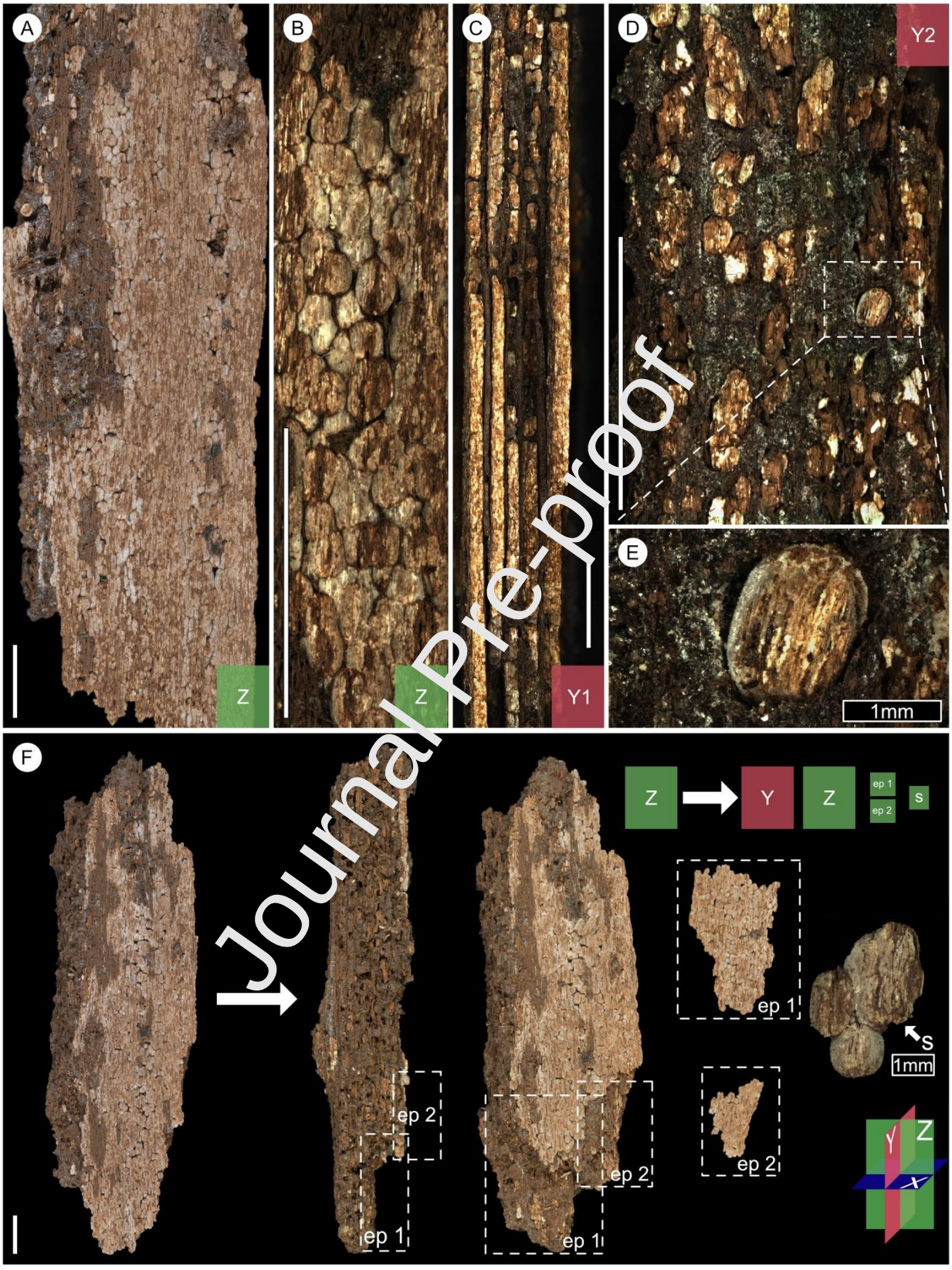

Figure 6

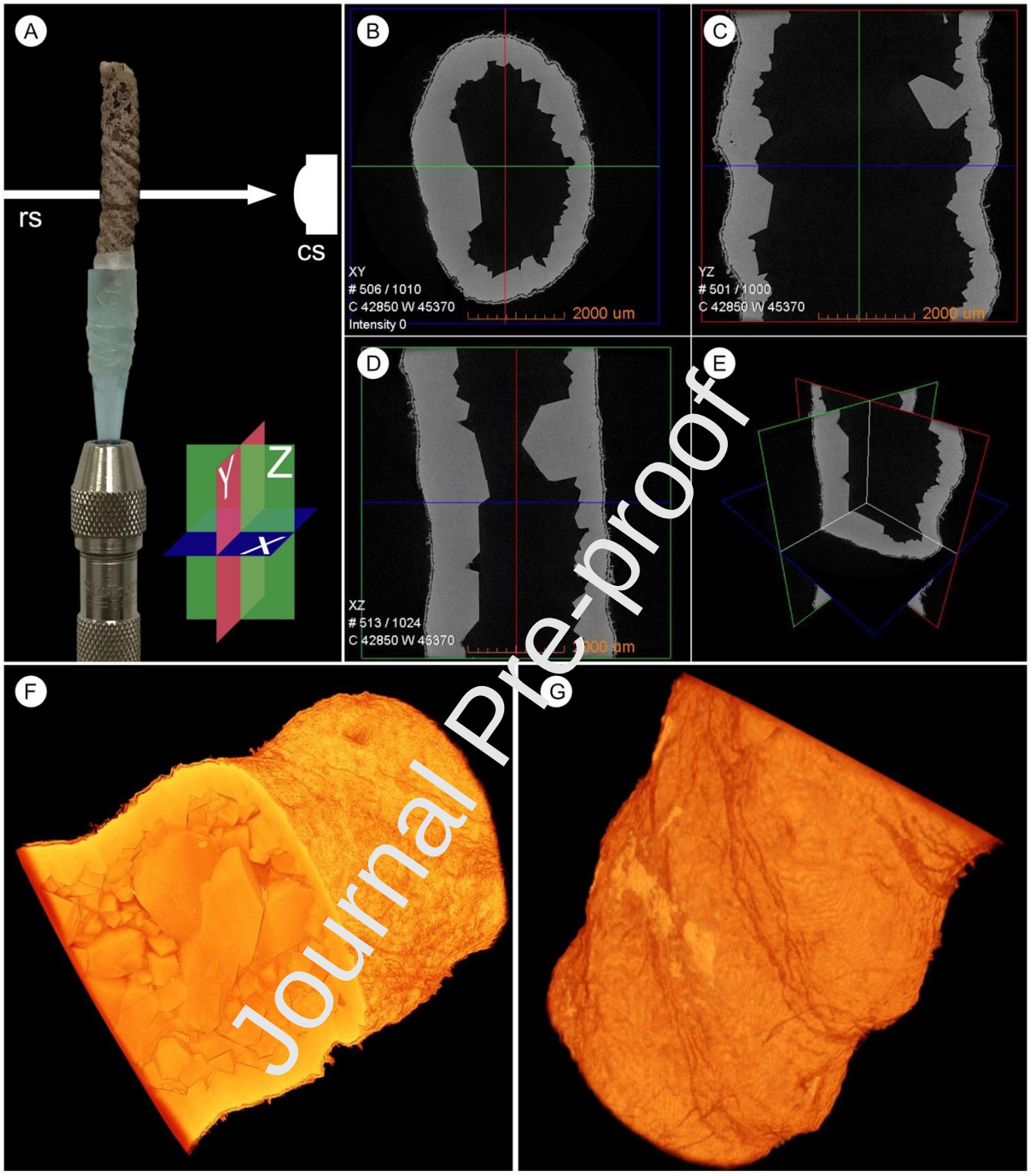

Figure 7

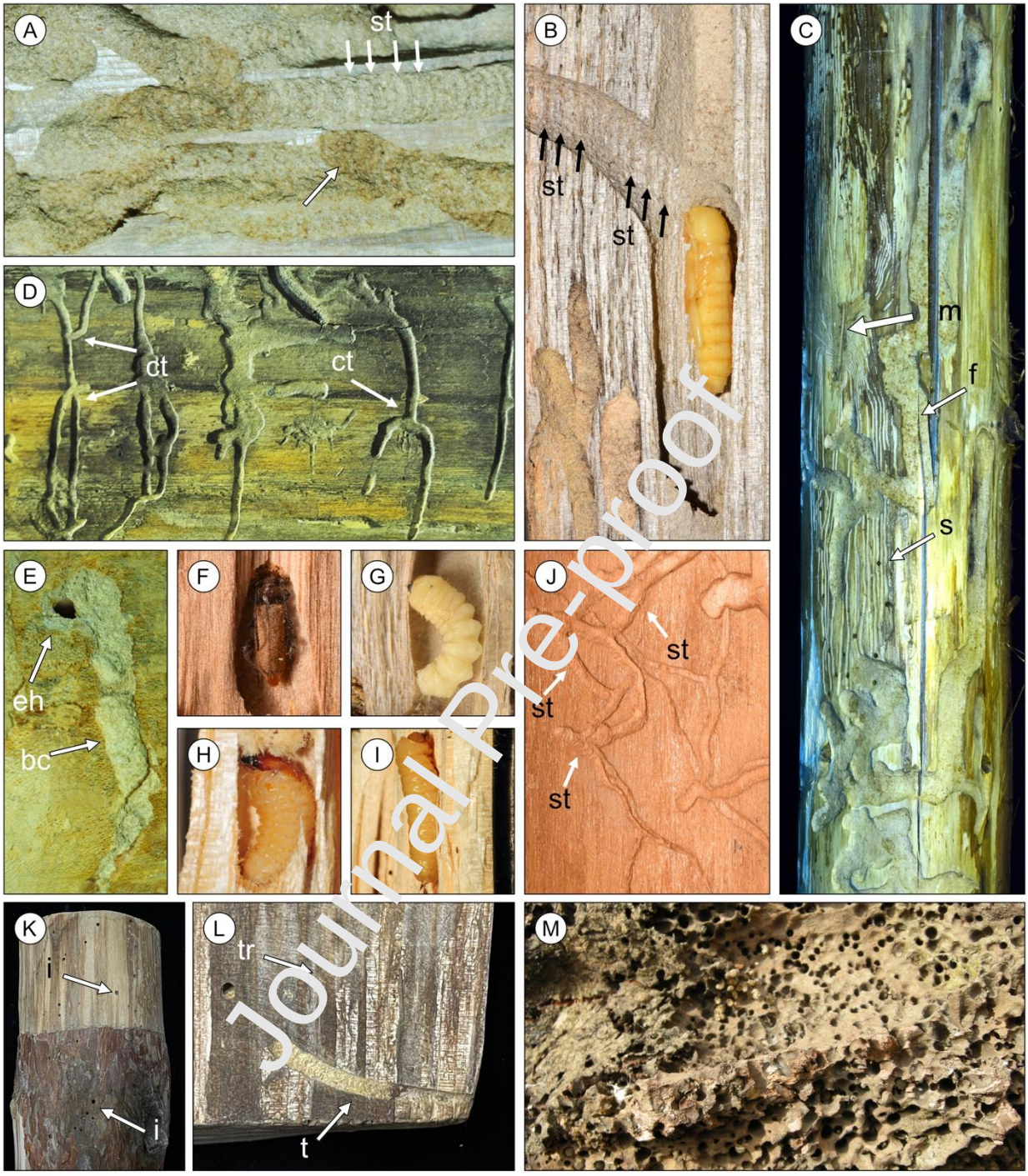

Figure 8

Figure 9

Samples	Features	Transverse section					Radial section			Tangential section		Reference
		Growth ring and wood transition	Transition from earlywood to latewood	Tracheid shape	Resin canal	Longitudinal parenchyma	Bordered pits in radial walls	Cross filed pitting	Ray height	Ray(s)	Transverse end walls of axial parenchyma	
Cryptomeria japonica	Evergreen	Distinct	Gradual	Polygonal to rectangular	Absent	Diffuse and short tangential band	1 row (occasionally 2 rows)	Taxodioid, 1–6, 1–2 rows	1–24 cells (23~358 μm)	Uniseriate, rarely partly biseriate	smooth	Jiang et al., 2010
Taxodium distichum	Deciduous	Distinct	Gradual	Irregular polygonal to rectangular	Absent	Diffuse	1–2 rows (mainly 2 rows, opposite in 2 rows)	Piciform, 2–4 , 1 (rarely 2) rows (s)	1–26 cells (–)	Mostly Uniseriate	smooth or distinct nodular	Jiang et al., 2010
Cunninghamia lanceolata	Evergreen	Distinct	Gradual	Irregular polygonal to square	Absent	Diffuse and tangential band	1 row (occasionally 2 rows)	Taxodioid, 1–6, 1–2 (rarely 3) rows	1–21 cells (~348 μm)	Uniseriate, relatively common biseriate	smooth or slightly nodular	Yi et al., 2003; Jiang et al., 2010
Glyptostrobus pensili	Deciduous (Except scale-like leaves)	Distinct	Gradual or slightly abrupt	Polygonal to rectangular or square	Absent	Diffuse and tangential band	2 rows mostly (occasionally 2 rows)	Taxodioid, 1–6, 1–2 (rarely 3) rows	1–35 cells (28~720 μm)	Uniseriate	smooth or slightly nodular	Jiang et al., 2010
Metasequoia glyptostroboides	Deciduous	Distinct	Slightly abrupt or abrupt	Irregular polygonal to rectangular	Absent	Diffuse	1 row (occasionally partly 2 rows)	Taxodioid, 1–6, 1 (rarely 2) row (s)	1–42 cells (30~870 μm)	Uniseriate	smooth or slightly nodular	Jiang et al., 2010
Sequoia sempervirens	Evergreen	Distinct	Abrupt	Irregular polygonal to rectangular	Absent	Diffuse, but concentrated in tangential zones	2–3 rows (mainly 2 rows, opposite)	Taxodioid, 1–4, 1–2 rows	1–40 cells (–)	Uniseriate	smooth	Jiang et al., 2010
Taiwania cryptomerioides	Evergreen	Distinct	Slightly abrupt or abrupt	Irregular polygonal to rectangular	Absent	Diffuse	1–2 rows (mostly 1 row)	Taxodioid, few cupressoid, 1–6, 1 (rarely 2) row(s)	1–29 cells (28~650 μm)	Uniseriate	smooth	Jiang et al., 2010
Taxodioxylon germanicum	–	Distinct	Abrupt	Polygonal	Absent	Diffuse, but concentrated in tangential zones	1–3 rows (mostly 2 rows)	Taxodioid 1–3, mostly arranged in pairs	1–20 cells (–)	Uniseriate, occasionally biseriate and homocellular	smooth	Erdei et al., 2009
Taxodioxylon szei	–	Distinct	Gradual	Polygonal to square	Absent	–	1–2 rows (opposite in 2 rows)	Taxodioid 1–6, 1–3 rows	1–50 cells (–)	Uniseriate, rarely partly biseriate	smooth	Yang and Zheng, 2003
Taxodioxylon cryptomeripsoides	–	Distinct	More or less Abrupt	rectangular or squarish	Absent	Diffuse	1 row (occasionally 2 rows)	Taxodioid, 1–4, 1–2 rows	1–18 (70% shows 3–12) cells	Uniseriate, rarely partly biseriate	smooth	Yi et al., 2003
Taxodioxylon cunninghamioides	–	Distinct, some indistinct	Abrupt	rectangular or squarish, some slightly round	Absent	Diffuse or shown as tangentially aligned pairs	1–2 rows (opposite in 2 rows)	Taxodioid, 1–5, 1–2 rows	1–15 (usually 3–10) cells	Uniseriate, and sometimes biseriate	smooth	Yi et al., 2003
Taxodioxylon sp.	Inferred deciduous (See 5.3)	Distinct	Abrupt	Polygonal to rectangular	Absent	Diffuse	1–2 rows (mainly 2 rows, opposite in 2 rows)	Taxodioid, 1–3, 1 (rarely 2) row (s)	6–28 (18) cells (–)	Uniseriate, rarely partly biseriate	smooth or slightly nodular	(This study)

Appendix A

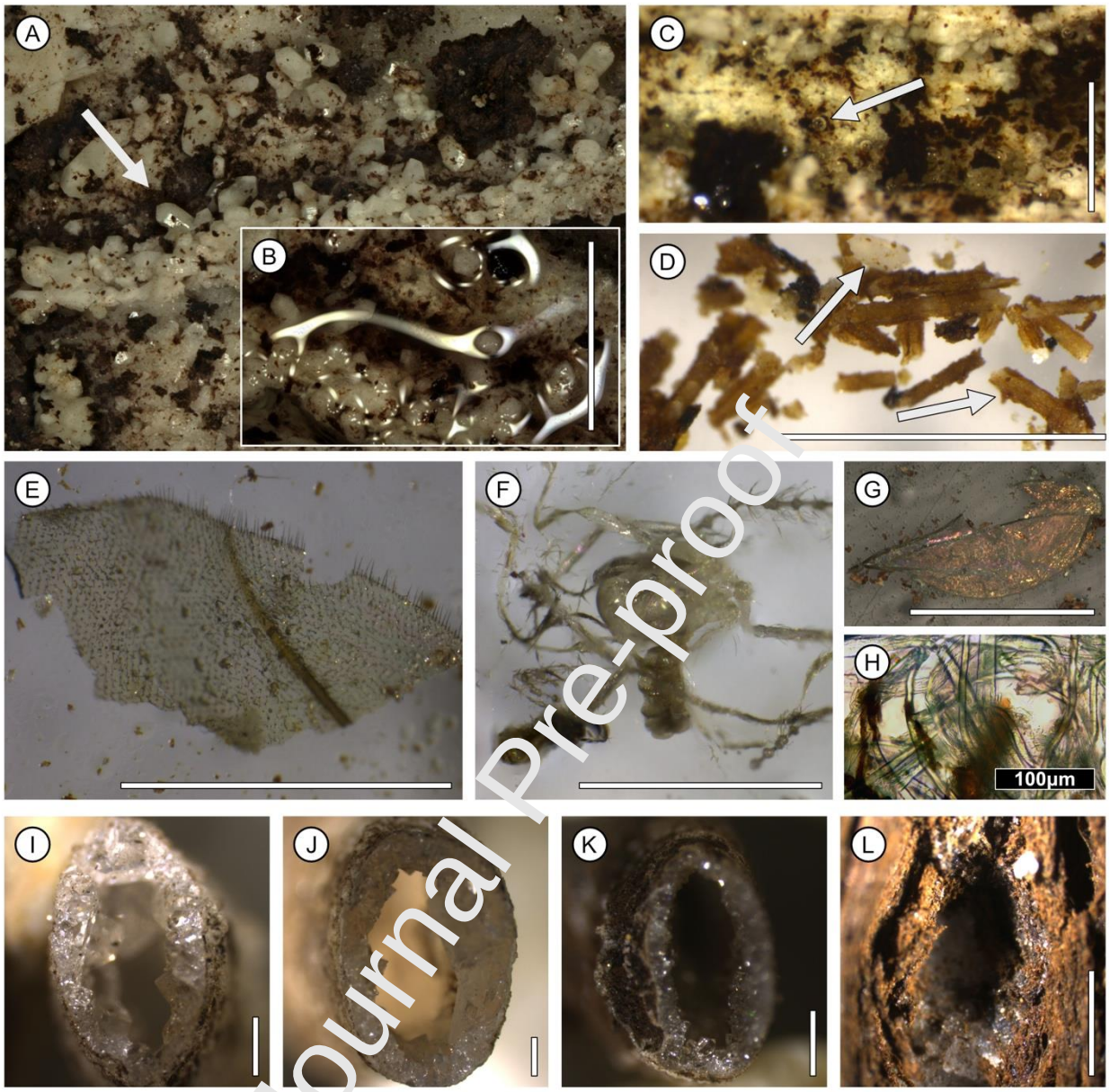

References

Bureau of Geology and Mineral Resources of Yunnan Province. 1996. Multiple Classification and Correlation of the Stratigraphy of China. Wuhan: China University of Geosciences Press. (In Chinese)

Carlquist, S., Nazaire, M., 2016. SEM studies of two riparian New-Caledonian conifers reveal air channels in stem wood; field observations. ALISO 34, 1–7.

Chen, C.J., 1990. The species, geographic distribution and biological characteristics of pine caterpillar in China. Integrated Management of Pine Caterpillar in China, 518.

Cope, J., 1984. Notes on the ecology of western Cerambycidae. Coleopt. Bull. 27–36.

Deng, W.Y.D., Su, T., Wappler, T., Liu, J., Li, S.F., Huang, J., Tang, H., Low, S.L., Wang, T.X., Xu, H., Xu, X.T., Liu, P., Zhou, Z.K., 2020. Sharp changes in plant diversity and plant-herbivore interactions during the Eocene–Oligocene transition on the southeastern Qinghai–Tibetan Plateau. Glob. Planet. Change 194, 103293.

Ding, W.N., Huang, J., Su, T., Xing, Y.W., Zhou, Z.K., 2018. An early Oligocene occurrence of the palaeoendemic genus *Dipteronia* (Sapindaceae) from Southwest China. Rev. Palaeobot. Palyno. 249, 16–23.

Dolezych, M., Schneider, W., 2007. Taxonomie und Taphonomie von Koniferenhölzern und Cuticulae dispersae im 2. Lausitzer Flözhorizont (Miozän) des Senftenberger Reviers. Palaeontographica Abt. B, 276 (1-3), 1-95. (In German)

Duan, H., Guo, J.B, Xuan, L., Wang, Z.Y, Li, M.Z, Yin, Y.L, Yang, Y., 2020. Comparative chloroplast genomics of the genus *Taxodium*. BMC Genom. 21 (1), 1–14.

Edmunds, G.F, McCafferty, W.P, 1996. New field observations on burrowing in Ephemeroptera from around the world. Entomol. News 107, 68–76.

Erdei, B., Dolezych, M., Hably, L., 2009. The buried Miocene forest at Bükkábrány, Hungary. Rev. Palaeobot. Palyno. 155 (1–2), 69–79.

Feng, Z., Wang, J., Rößler, R., Ślipiński, A., Labandeira, C., 2017. Late Permian wood-borings reveal an intricate network of ecological relationships. Nat. Commun. 8 (1), 1–6.

Fierke, M K, Kinney, D N, Salisbury, V.B., Crook, D.J., Stephen, F M, 2005 Development and comparison of intensive and extensive sampling methods and preliminary within-tree population estimates of red oak borer (Coleoptera Cerambycidae) in the Ozark Mountains of Arkansas. Environ. Entomol. 34, 184–192

Francis, J.E., Harland, B.M., 2006. Termite borings in Early Cretaceous fossil wood, Isle of Wight, UK. Cretaceous Res. 27 (6), 773–777.

Genise, J.F., 2004. Fungus traces in wood: a rare bioerosional item. Ichnia. 37, 19–23.

Genise, J.F., Garrouste, R., Nel, P., Grandcolas, P., Maurizot, P., Cluzel, D., Cornette, R., Fabre, A.C., Nel, A., 2012. *Asthenopodichnium* in fossil wood. Different trace makers as indicators of different terrestrial palaeoenvironments. Palaeogeogr. Palaeoclimatol. Palaeoecol. 365, 184–191.

Greguss, P., 1955. Identification of living gymnosperms on the basis of xylotomy. Identification of living gymnosperms on the basis of xylotomy. Akademiai Kiado.

Grehan, J.R, 1987. Life cycle of the wood-borer *Aenetus virescens* (Lepidoptera: Hepialidae). New Zeal. J. Zool. 14 (2), 209–217.

Greppi, C.D., Massini, J.L.G., Fujana, R.R., 2021. Saproxylic arthropod borings in *Nothofagoxylon* woods from the Miocene of Patagonia. Palaeogeogr. Palaeoclimatol. Palaeoecol. 571, 110369.

Han, Y., Shih, C.K., Ren, D., Wang, Y.J., 2022. New wood soldier flies from mid-Cretaceous Myanmar amber (Diptera, Stratiomyomorpha, Xylomyidae). Cretac. Res. 105142.

Hartig, T., 1848. Beiträge zur Geschichte der Pflanzen und zur Kenntnis der norddeutschen Braunkohlen-Flora. Bot. Ztg. 6 (10), 185–190. (In German)

Huang, Y.J., Jacques, F.M., Su, T., Ferguson, D.K., Tang, H., Chen, W.Y., Zhou, Z.K., 2015. Distribution of Cenozoic plant relicts in China explained by drought in dry season. Sci. Rep. 5 (1), 1–7.

Hulcr, J., Dunn, R.R., 2011. The sudden emergence of pathogenicity in insect–fungus symbioses threatens naive forest ecosystems. P. Roy. Soc. B-Biol. Sci. 278 (1720), 2866–2873.

InsideWood. 2004-onwards. Published on the Internet. http://insidewood.lib.ncsu.edu/search [2021].

Jiang, X.M., Cheng, M.Y., Ying, Y.F., 2010. Atlas of Gymnosperms Woods of China. Science Press. (In Chinese with English translation)

Kimoto, T., Duthie-Holt, M., 2004. Exotic Forest Insect Guidebook. Plant Pest Survey Unit, Canadian Food Inspection Agency.

Kluge, N., 2013. The phylogenetic system of Ephemeroptera. Springer Science & Business Media.

Kruse, J.J., 2000. *Archips goyeriana*, n. sp. (Lepidoptera: Tortricidae) an important pest of baldcypress (Taxodiaceae) in Louisiana and Mississippi. Proc. Entomol. Soc. Wash. 102 (3), 741–746.

Kubitzki, K., Rohwer, J.G., Bittrich, V., 1990. The families and genera of vascular plants. Springer.

Kus, J., Dolezych, M., Schneider, W., Hofmann, T., Rajczi, E.V., 2020. Coal petrological and xylotomical characterization of Miocene lignites and *in-situ* fossil tree stumps and trunks from Lusatia region, Germany: Palaeoenvironment and taphonomy assessment. Int. J. Coal Geol. 217, 103283.

Labandeira, C.C., Phillips, T.L., Norton, R.A., 1997. Oribatid mites and the decomposition of plant tissues in Paleozoic coal-swamp forests. Palaios 12 (4), 319–353.

Labandeira, C.C., Phillips, T.L., 2002. Stem borings and petiole galls from Pennsylvanian tree ferns of Illinois, USA: implications for the origin of the borer and galler functional-feeding-groups and holometabolous insects. Palaeontographica Abt. A 264, 1–84.

Labandeira, C.C, 2014. Why Did Terrestrial Insect Diversity Not Increase During the Angiosperm Radiation? Mid-Mesozoic, Plant-Associated Insect Lineages Harbor Clues, in: Pontarotti, P. (Ed.), Evolutionary Biology: Genome Evolution, Speciation, Coevolution and Origin of Life. Springer International Publishing, Cham, pp. 261–299.

Leskey, T.C., Christopher Bergh, J., Walgenbach, J.F., Zhang, A.J., 2009. Evaluation of pheromone-based management strategies for dogwood borer (Lepidoptera: Sesiidae) in commercial apple orchards. J. Econ. Entomol. 102 (3), 1085–1093.

Li, S.H., Su, T., Spicer, R.A., Xu, C.L., Sherlock, S., Halton, A., Hoke, G., Tian, Y.M., Zhang, S.T., Zhou, Z.K., Deng, C.L., Zhu, R.X., 2020. Oligocene deformation of the Chuandian terrane in the SE margin of the Tibetan Plateau related to the extrusion of Indochina. Tectonics, 39 (7), e2019TC005974.

Lieutier, F., Day, K.R., Battisti, A., Grégoire, J.C., Evans, H.F., 2004. Bark and Wood Boring Insects in Living Trees in Europe: a Synthesis. Springer.

Linnemann, U., Su, T., Kunzmann, L., Spicer, R.A., Ding, W.N., Spicer, T.E.V., Zieger, J., Hofmann, M., Moraweck, K., Gärtner, A., Gerdes, A., Marko, L., Zhang, S.T., Li, S.F., Tang, H., Huang, J., Mulch, A., Mosbrugger, V., Zhou Z.K., 2017. New U-Pb dates show a Paleogene origin for the modern Asian biodiversity hot spots. Geology 46 (1), 3–6.

Lonsdale, D., Pautasso, M., Holdenrieder, O., 2008. Wood-decaying fungi in the forest: conservation needs and management options. Eur. J. For. Res. 127 (1), 1–22.

Luczaj, J.A., Leavitt, S.W., Csank, A.Z., Panyushkina, I.P., Wright, W.E., 2018. Comment on "Non-mineralized fossil wood" by George E. Mustoe (Geosciences, 2018). Geosciences 8 (12), 462.

Ma Q.W., Xu J.X., Wang Y.F., Li C.S., 2000. First evidence of Sequoia in the Miocene of Yunnan province, China. Acta bot. Sin. 42 (4), 438–440. (In Chinese with English Abstract)

McLoughlin, S., Mays, C., 2022. Synchrotron X-ray imaging reveals the three-dimensional architecture of beetle borings (Dekosichnus meniscatus) in Middle-Late Jurassic araucarian conifer wood from Argentina. Rev. Palaeobot. Palynol. 297, 104568

Moran, K., Hilbert-Wolf, H.L., Golder, K., Malenda, H.F., Smith, C.J., Storm, L.P., Simpson, E.L., Wizevich, M.C., Tindall, S.E., 2010. Attributes of the wood-boring trace fossil

Asthenopodichnium in the Late Cretaceous Wahweap Formation, Utah, USA. Palaeogeogr. Palaeoclimatol. Palaeoecol. 297 (3–4), 662–669.

Morgan, F.D., 1968. Bionomics of siricidae. Annu. Rev. Entomol. 13 (1), 239–256.

Mustoe, G.E., 2018. Non-mineralized fossil wood. Geosciences 8 (6), 223.

Mustoe, G.E., Viney, M., Mills, J., 2019. Mineralogy of Eocene fossil wood from the "Blue Forest" locality, southwestern Wyoming, United States. Geosciences 9 (1), 35.

Naugolnykh, S.V., Ponomarenko, A.J., 2010. Possible traces of feeding by beetles in coniferophyte wood from the Kazanian of the Kama River basin. Paleontol. J. 44 (4), 468–474.

Norton, R.A., Bonamo, P.M., Grierson, J.D., and Shear, W.A., 1993. Oribatid mite fossils from a terrestrial Devonian deposit near Gilboa, New York. J. Paleontol. 62 (2), 259–269.

Ohya, E., Ogura, N., 1993. Rearing of the cypress bark moth, *Epinotia granitalis* (Butler) (Lepidoptera: Tortricidae) on artificial diets. J. Jpn. For. Soc. 75 (6), 561–563.

Ortega-Blanco, J., Rasnitsyn, A.P., Delclòs, X., 2008. First record of anaxyelid woodwasps (Hymenoptera: Anaxyelidae) in Lower Cretaceous Spanish amber. Zootaxa 1937 (1), 39–50.

Philippe, M., Bamford, M.K., 2008. A key to morphogenera used for Mesozoic conifer-like woods. Rev. Palaeobot. Palynol. 148 (3–4), 184–207.

Richter, H.G., Grosser, D., Heinz, I., Gasson, P.E., 2004. IAWA list of microscopic features for softwood identification. IAWA J. 25, 1–70.

Solomon, J.D., 1977. Frass characteristics for identifying insect borers (Lepidoptera: Cossidae and Sesiidae; Coleoptera: Cerambycidae) in living hardwoods. Can. Entomol. 109 (2), 295–303.

Stidd, B.M., Phillips T.L., 1982. *Johnhallia lacunosa* gen. et sp. n.: a new pteridosperm from the Middle Pennsylvanian of Indiana. J. Paleontol. 56 (5), 1093–1102.

Stokland, J.N., Siitonen, J., Jonsson, B.G., 2012. Biodiversity in Dead Wood. Cambridge University Press.

Sun, B.N., Wu, J.Y., Liu, Y.S.C., Ding, S.T., Li, X.C., Xie, S.P., Yan, D.F., Lin, Z.C., 2011. Reconstructing Neogene vegetation and climates to infer tectonic uplift in western Yunnan, China. Palaeogeogr. Palaeoclimatol. Palaeoecol. 304 (3–4), 328–336.

Su, T., Liu, Y.S., Jacques, F.M.B., Huang, Y.J., Xing, Y.W., Zhou, Z.K., 2013. The intensification of the East Asian winter monsoon contributed to the disappearance of *Cedrus* (Pinaceae) in southwestern China. Quat. Res. 80 (2), 316–325.

Su, T., Spicer, R.A., Li, S.F., Xu, H., Huang, J., Sarah, A., Huang, Y.J., Li, S.H., Wang, L., Jia, L.B., Deng, W.Y.D., Liu, J., Deng, C.L., Zhang, S.T., Paul, J.V., Zhou, Z.K, 2019. Uplift, climate and biotic changes at the Eocene–Oligocene transition in South-Eastern Tibet. Natl. Sci. Rev. 6 (3), 495–504.

Sutherland, J.I., 2003. Miocene petrified wood and associated borings and termite faecal pellets from Hukatere Peninsula, Kaipara Harbour, North Auckland, New Zealand. J. R. Soc. N. Z. 33 (1), 395–414.

Tang, H., Li, S.F., Su, T., Spicer, R.A., Zhang, S.T., Li, S.H., Liu, J., Lauretano, V., Witkowski, C.R., Spicer, T.E.V., Deng, W.Y.D., Wu, M.X., Ding, W.N., 2020. Early Oligocene vegetation and climate of southwestern China inferred from palynology. Palaeogeogr. Palaeoclimatol. Palaeoecol. 560, 109988.

Thenius, E., Klaus, W., 1978. Lebensspuren von Ephemeropteren-Larven aus dem Jung-Tertiär des Wiener Beckens. Ann. Naturhistor. Mus. Wien 82, 177–188. (In German)

Yi, T.M., Li, C.S., Xu, J.X., 2003. Late Miocene woods of Taxodiaceae from Yunnan, China. J. Integr. Plant Biol. 45 (4), 384. (In Chinese)

Uchman, A., 2011. Recent freshwater wood borings from the Vistula River in Poland, 7th International Bioerosion Workshop, Faial, Azores, pp. 18–23.

Villari, C., Herms, Herms D.A., Whitehill J.G.A., Cipollini, D., Bonello, P., 2015. Progress and gaps in understanding mechanisms of ash tree resistance to emerald ash borer, a model for wood-boring insects that kill angiosperms. 2016. New Phytol. 209 (1), 63–79.

Walter, D.E., Proctor, H.C., 1999. Mites: Ecology, Evolution, and Behaviour. Springer.

Wang L., Kunzmann L., Su T., Xing Y.W., Zhang S.T., Wang Y.Q., Zhou Z.K., 2013. The disappearance of *Metasequoia* (Cupressaceae) after the middle Miocene in Yunnan, Southwest China: Evidences for evolutionary stasis and intensification of the Asian monsoon. Rev. Palaeobot. Palynol. 264, 64–74

Wei H.B., Gou X.D., Yang J.Y., Feng Z., 2019. Fungi–plant–arthropods interactions in a new conifer wood from the uppermost Permian of China reveal complex ecological relationships and trophic networks. Palaeogeogr. Palaeoclimatol. Palaeoecol. 271, 104100.

Wheeler, E.A., 2011. Inside Wood–A web resource for hardwood anatomy. IAWA J. 32 (2), 199–211.

Wood, D.L., Koerber, T.W., Scharpf, R.F., Storer, A.J., 2003. Pests of the Native California Conifers. University of California Press.

Wu, J., Zhang, K.X., Xu, Y.D., Wang, G.C., Garzione, C.N., Eiler, J., Leloup, P.H., Sorrel, P., Mahéo, G., 2018. Paleoelevations in the Jianchuan Basin of the southeastern Tibetan Plateau based on stable isotope and pollen grain analyses, Palaeogeogr., Palaeoclim., Palaeoecol., 510, 93–108,

Xu, J.X., Ferguson, D.K., Li, C.S., Wang, Y.F., 2008. Late Miocene vegetation and climate of the Lühe region in Yunnan, southwestern China. Rev. Palaeobot. Palyno. 148 (1), 36–59.

Yang X.J., Zheng S.L., 2003. A new species of *Taxodioxylon* from the Lower Cretaceous of the Jixi Basin, eastern Heilongjiang, China. Cretac. Res. 24 (6), 653–660.

Zhang, J.W., D'Rozario A., Adams J.M., Li Y., Liang X.Q., Jacques, F.M.B., Su T., Zhou Z.K., 2015. *Sequoia maguanensis*, a new Miocene relative of the coast redwood, *Sequoia* sempervirens, from China: Implications for paleogeography and paleoclimate. Am. J. Bot. 102(1), 103–118

Zhang, H., 2017. Three-dimensional reconstruction of the galleries of several wood borer species. Beijing Forestry University. Master Thesis. (In Chinese)

Zhou, X.D., Beer, Z.W., Wingfield, M.J., 2013. Ophiostomatoid fungi associated with conifer-infesting bark beetles in China. CBS Biodiversity Series.

The authors declared that they have no conflicts of interest to this work.

Highlights

1, First report of extensive arthropod and fungal traces in the Oligocene Lühe flora.

2, Shows a new wood fossil record of *Taxodioxylon* in this region.

3, Enhances understanding of post-Oligocene climatic change in southwestern China.